Susceptibility and resilience to maternal immune activation are associated with differential expression of endogenous retroviral elements

Herrero, Felisa ; Mueller, Flavia S ; Gruchot, Joel ; Küry, Patrick ; Weber-Stadlbauer, Ulrike ; Meyer, Urs

DOI: https://doi.org/10.1016/j.bbi.2022.10.006

Brain, Behavior, and Immunity 107 (2023) 201–214

Contents lists available at ScienceDirect

Brain Behavior and Immunity

journal homepage: www.elsevier.com/locate/ybrbi

Susceptibility and resilience to maternal immune activation are associated with differential expression of endogenous retroviral elements

Felisa Herrero [a,1], Flavia S. Mueller [a,1], Joel Gruchot [b], Patrick Küry [b], Ulrike Weber-Stadlbauer [a,c], Urs Meyer [a,c,*]

[a] Institute of Pharmacology and Toxicology, University of Zurich-Vetsuisse, Zurich, Switzerland
[b] Department of Neurology, Medical Faculty, Heinrich-Heine-University Düsseldorf, Düsseldorf, Germany
[c] Neuroscience Center Zurich, University of Zurich and ETH Zurich, Zurich, Switzerland

ARTICLE INFO

Keywords:
Cytokines
Endogenous retroviruses
Inflammation
Maternal immune activation
Neurodevelopmental disorders
Resilience
Schizophrenia

ABSTRACT

Endogenous retroviruses (ERVs) are ancestorial retroviral elements that were integrated into the mammalian genome through germline infections and insertions during evolution. While increased ERV expression has been repeatedly implicated in psychiatric and neurodevelopmental disorders, recent evidence suggests that aberrant endogenous retroviral activity may contribute to biologically defined subgroups of psychotic disorders with persisting immunological dysfunctions. Here, we explored whether ERV expression is altered in a mouse model of maternal immune activation (MIA), a transdiagnostic environmental risk factor of psychiatric and neurodevelopmental disorders. MIA was induced by maternal administration of poly(I:C) on gestation day 12 in C57BL/6N mice. Murine ERV transcripts were quantified in the placentae and fetal brains shortly after poly(I:C)-induced MIA, as well as in adult offspring that were stratified according to their behavioral profiles. We found that MIA increased and reduced levels of class II ERVs and syncytins, respectively, in placentae and fetal brain tissue. We also revealed abnormal ERV expression in MIA-exposed offspring depending on whether they displayed overt behavioral anomalies or not. Taken together, our findings provide a proof of concept that an inflammatory stimulus, even when initiated in prenatal life, has the potential of altering ERV expression across fetal to adult stages of development. Moreover, our data highlight that susceptibility and resilience to MIA are associated with differential ERV expression, suggesting that early-life exposure to inflammatory factors may play a role in determining disease susceptibility by inducing persistent alterations in the expression of endogenous retroviral elements.

1. Introduction

Endogenous retroviruses (ERVs) are inherited retroviral genomic elements that integrated into the eukaryotic genome through germline infections and insertions during evolution (Feschotte and Gilbert, 2012). They belong to a family of genomic elements referred to as retrotransposons, which use a "copy-and-paste" mechanism to integrate their DNA product into the genome based on reverse transcription of an RNA intermediate (Bourque et al., 2018). It is estimated that human ERVs comprise 5–8 % of the human genome (Lander et al., 2001), which readily surpasses the 1–2 % of human DNA containing protein-coding sequences. ERVs are similarly abundant in other mammalian species and comprise, for example, approximately 10 % of the mouse genome (Waterston et al., 2002).

Under physiological conditions, the majority of ERVs are thought to be in a dormant state and suppressed by molecular mechanisms mediating epigenetic silencing. The latter involves intricate interactions between DNA methylation, histone modifications and non-coding RNAs (Geis and Goff, 2020). Upon exposure to certain environmental stimuli such as infection or stress, however, dormant ERVs can become activated and may contribute to a number of pathologies, including autoimmune disorders (Volkman and Stetson, 2014), cancer (Kassiotis, 2014), and neurological disorders (Küry et al., 2018). Increased expression of ERVs have also been repeatedly found in neurodevelopmental and psychiatric disorders (Balestrieri et al., 2019b; Misiak et al., 2019), including schizophrenia (Karlsson et al., 2004;

* Corresponding author at: Institute of Pharmacology and Toxicology, University of Zurich-Vetsuisse, Winterthurerstrasse 260, 8057 Zurich, Switzerland.
E-mail address: urs.meyer@vetpharm.uzh.ch (U. Meyer).
[1] Shared first authorship.

https://doi.org/10.1016/j.bbi.2022.10.006
Received 3 June 2022; Received in revised form 26 September 2022; Accepted 9 October 2022
Available online 12 October 2022

Perron et al., 2008; 2012; Yao et al., 2008; Li et al., 2019), bipolar disorder (Perron et al., 2012), autism spectrum disorders (ASD) (Balestrieri et al., 2012; 2019a), and attention deficit hyperactivity disorder (ADHD) (Balestrieri et al., 2014; Cipriani et al., 2018a). Intriguingly, high levels of ERV transcripts are only found in certain subgroups of neurological or psychiatric patients, especially in those that display signs of chronic inflammation (Balestrieri et al., 2019a; Tamouza et al. 2021). Hence, aberrant endogenous retroviral activity may contribute to biologically defined subgroups of brain disorders with persisting immunological dysfunctions.

In the present study, we explored whether the expression of endogenous retroviral elements is altered in a mouse model of maternal immune activation (MIA). Our rationale for these investigations was twofold. First, infectious and non-infectious MIA has been repeatedly implicated in the etiology of neurodevelopmental and psychiatric disorders (Brown and Meyer, 2018; Pollak and Weber-Stadlbauer, 2020), but it is currently unknown whether this association involves alterations in ERV expression. Second, although MIA has been established as a risk factor for neurodevelopmental and psychiatric disorders, a substantial portion of offspring exposed to MIA is resilient to this early-life adversity and does not develop overt pathologies (Meyer, 2019). Consistent with the latter notion, we recently identified the existence of subgroups of MIA-exposed offspring that show dissociable behavioral, transcriptional, brain network and inflammatory profiles even under conditions of genetic homogeneity and identical MIA in the mouse species (Mueller et al., 2021). Extending our research to the profiling of ERV expression in the MIA model may thus offer additional insights into the molecular mechanisms underlying the dissociation of MIA-exposed offspring into susceptible and resilient subgroups.

In our study, MIA was induced by maternal administration of poly(I:C) during pregnancy in mice. Poly(I:C) is a synthetic analog of double-stranded RNA that induces a cytokine-associated viral-like acute phase response and is widely used in immune-mediated neurodevelopmental disruption models as applied to mice (Meyer, 2014; Kentner et al., 2019) and other species (Careaga et al., 2017; Weber-Stadlbauer and Meyer, 2019). Importantly, we recently explored trait variability in the poly(I:C)-based MIA model in mice, revealing marked differences between individual MIA offspring in terms of their behavioral and neuroanatomical profiles (Mueller et al., 2021). Thus, this model offers an opportunity to examine whether the variable behavioral effects of MIA are related to a varying expression of ERVs. To this end, we quantified murine ERV transcripts in the placentae and in fetal brains shortly after poly(I:C)-induced MIA, as well as in adult offspring that were stratified according to the presence (susceptible) or absence (resilient) of behavioral deficits. Placental tissue as well as fetal and adult brain samples were obtained from male and female offspring and were analyzed separately in order to identify possible sex differences.

The profiling of ERV expression involved the quantification of several class II murine ERVs (Lueders and Kuff, 1980; Wicker et al., 2007), including the type II early transposon I (ETnI), IIα (ETnIIα), and IIβ (ETnIIβ), as well as intracisternal A-particle (IAP) and mouse type D retrovirus (MusD). While the precise physiological functions of these ERVs remain largely unknown, it has been shown that IAP is able to transpose through retroviral mechanisms in the cisternae of the endoplasmic reticulum (Lueders and Kuff, 1980) and to modulate the transcriptional activity of neighboring genes (Sharif et al., 2013), providing functional promoter elements and shaping local epigenetic landscapes through changes in DNA methylation and histone modifications. On the other hand, MusD is believed to mediate the retrotransposition of ETn transcripts by providing MusD gene-encoded reverse transcriptase and other proteins (Mager and Freeman, 2000). Hence, MusD appears to facilitate the retrotransposons activity of ETn transcripts and may be responsible for a substantial proportion of the insertional mutagenesis in the mouse germ line (Maksakova et al., 2006). The rationale underlying the selection of the class II murine ERVs was twofold. First, they are phylogenetically related to the human ERV-K (HERV-K) elements (Stocking and Kozak, 2008), which in turn have been found to be increased in various psychiatric and neurodevelopmental disorders, including schizophrenia (Frank et al., 2005; Slokar and Hasler, 2016), bipolar disorder (Frank et al., 2005) and ASD (Tovo et al., 2022). Second, high expression of class II murine ERVs has been found in two mouse models relevant for ASD (Cipriani et al., 2018b), suggesting that they may play a role in altering brain development and functions implicated in ASD.

In addition to class II murine ERVs, we also quantified syncytin-A (SynA) and syncytin-B (SynB), which are the murine analogues to human syncytin-1 (Syn1) and syncytin-2 (Syn2), respectively (Dupressoir et al., 2005). Syncytins share many structural elements with class I retroviral glycoproteins and belong to the class I ERVs, which also contain human ERV type-W (HERV-W) elements (Wicker et al., 2007). While syncytins are pivotal for placental development and maintenance of pregnancy (Mi et al., 2000; Dupressoir et al., 2011), they have been found to have pro-inflammatory effects in the adult central nervous system (Wang et al., 2018a; b). Furthermore, increased expression of syncytin transcripts has been found in some cases with schizophrenia (Perron et al., 2008; Huang et al., 2011; Wang et al., 2018b), providing a rationale for their inclusion in the current study.

We also assessed the transcripts of interleukin-6 (IL-6) in placental tissue and in fetal and adult brain samples in order to identify possible correlations between the expression of ERV transcripts and a MIA-associated key cytokine (Smith et al., 2007; Hsiao and Patterson, 2011; Aguilar-Valles et al., 2012). In addition, we quantified IL-6 protein in maternal plasma and investigated possible relationships between maternal IL-6 levels and alterations in placental and fetal ERV expression.

2. Materials and methods

2.1. Animals

C57BL/6N mice were used throughout the whole study. Female and male breeder mice were obtained from Charles River Laboratories (Sulzfeld, Germany) at the age of 10 weeks. Upon arrival, they were housed in individually ventilated cages (IVCs; Allentown Inc., Bussy-Saint-Georges, France) as described in detail before (Mueller et al., 2018a). The cages were kept in a specific-pathogen-free (SPF) holding room, which was temperature- and humidity-controlled (21 ± 3 °C, 50 ± 10 %) and kept under a reversed light–dark cycle (lights off: 09:00 AM–09.00 PM). All animals had *ad libitum* access to standard rodent chow (Kliba 3336, Kaiseraugst, Switzerland) and water throughout the entire study. All procedures had been previously approved by the Cantonal Veterinarian's Office of Zurich, Switzerland.

2.2. Breeding and maternal manipulations

Timed-pregnant mice were generated via on-site breeding, which began two weeks after the animals were acclimatized to our facility. To this end, female and male breeders were subjected to a timed-mating procedure as previously described (Mueller et al., 2018a; 2019). Successful mating was verified by the presence of a vaginal plug, upon which dams were housed individually throughout gestation. The presence of a vaginal plug was referred to as gestational day GD 0. A dam showing a vaginal plug at GD 0 and a weight gain of ≥3 g from GD 0 to GD 12 was considered as undergoing successful pregnancy (Mueller et al., 2019).

On GD 12, pregnant mice were randomly assigned to a single injection of poly(I:C) (potassium salt, P9582, Sigma–Aldrich, Buchs, St Gallen, Switzerland) or treatment with pyrogen-free 0.9 % NaCl (B. Braun, Melsungen, Switzerland) vehicle solution. We previously ascertained the quality, molecular composition and immunopotency of the poly(I:C) batch (#086M4045V) used in this study (Mueller et al., 2019). Based on our previous dose–response studies (Mueller et al., 2018a) and

molecular composition of the poly(I:C) batch, poly(I:C) was administered intravenously (i.v.) into the tail vein at a dose of 5 mg/kg. The dose of poly(I:C) was calculated based on the pure form and was dissolved in glass vials with vehicle (sterile 0.9 % saline solution) kept at room temperature. Control (CON) dams received vehicle solution (i.v.) only. All solutions were freshly prepared on the day of their administration and injected using an injection volume of 5 ml/kg. The tail vein injections were performed under mild physical constraint using a semi-restrictive rodent injection cone (model 561-RC; Plas-Labs Inc., Lansing, USA). Immediately after poly(I:C) or vehicle administration, the dams were placed back to their home cages and left undisturbed until collection of placental and fetal samples 6 hrs after the maternal treatment on GD 12 (cohort 1; *N*[CON dams] = 5, *N*[MIA dams] = 5), or until 7 days after birth (cohort 2; *N*[CON dams] = 8, *N*[MIA dams] = 8).

Offspring born to CON and MIA dams were weaned on postnatal day (PND) 21, and littermates of the same sex were caged separately and maintained in groups of 3 to 5 animals per cage. Additional methodological details regarding the maternal manipulations are summarized in the reporting guideline checklist for the MIA model (Kentner et al., 2019), as provided in Supplementary Table S1.

2.3. Collection of maternal, placental and fetal tissues

Maternal plasma, placentae and fetal brain tissue (cohort 1) were collected 6 h after poly(I:C) or vehicle treatment. Pregnant mice were decapitated using surgical scissors without prior anesthesia, and trunk blood was collected into Eppendorf tubes containing ethylenediaminetetraacetic acid (EDTA). The collected blood was kept on ice for a maximum of 30 min before centrifugation (2000 × *g*, 10 min) to collect plasma, which was stored at −20 °C until further use. Placental and fetal brain tissues were collected as described before (Mueller et al., 2019). In brief, the abdominal cavity was exposed to collect the uterine horns, which were placed into a petri dish filled with ice-cold PBS. Decidual tissue and yolk sac were then removed for individual fetuses, and the fetuses were further dissected to obtain fetal brain tissue according to landmarks provided before (Mueller et al., 2019). Subsequently, the isolated fetal brain and placental tissues were placed in Eppendorf tubes, snap-frozen by immersion in liquid nitrogen, and stored at −80 °C until further use. The sex of each of the fetal and corresponding placental sample was determined using PCR to detect male-specific sequence (Sry) according to previously established protocols (Lambert et al., 2000). For each CON or MIA dam, one fetal and one placental sample per sex (*N*[CON fetuses/placentae] = 5 per sex, *N*[MIA fetuses/placentae] = 5 per sex) were assigned to the subsequent assessment of ERV and IL-6 expression (see below).

2.4. Behavioral testing

Behavioral testing commenced when CON and MIA offspring (cohort 2) reached 12 weeks of age and included tests for social interaction and prepulse inhibition (PPI) of the acoustic startle reflex (see below). These tests were selected because of their relevance to neurodevelopmental disorders (Meyer et al., 2009; Silverman et al., 2010) and because they can discriminate MIA-exposed offspring displaying behavioral deficits from MIA-exposed offspring showing no overt behavioral deficits in adulthood (Mueller et al., 2021). Offspring from both sexes were included in the behavioral testing, with males and females tested on separate days. For each sex, *N* = 8 CON originating from 8 litters and *N* = 16 MIA offspring originating from 8 litters were randomly selected for behavioral testing. This sample size was selected based on previous findings (Mueller et al., 2021), showing that 40–60 % of the offspring from a MIA-exposed litter display overt deficits in the social interaction and PPI tests (susceptible offspring; Sus-MIA subgroup), whereas the remaining offspring do not (resilient offspring; Res-MIA subgroup). All animals were first assigned to the social interaction test, followed by the PPI test, using a testing-free resting period of 4 days between the two tests.

2.4.1. Social interaction test

Social interaction was assessed by analyzing the relative exploration time between an unfamiliar congenic mouse and an inanimate dummy object using methods established before (Mueller et al., 2018a; 2021). The test apparatus was made of Plexiglas and consisted of three identical arms (50 cm × 9 cm; length × width) surrounded by 10-cm high Plexiglas walls. The three arms radiated from a central triangle (8 cm on each side) and spaced 120° from each other. Two out of the three arms contained a rectangular wire grid cage (13 cm × 8 cm × 10 cm, length × width × height; bars horizontally and vertically spaced 9 mm apart). The third arm did not contain a metal wire cage and served as the start zone.

All animals were first habituated to the test apparatus on the day before social interaction testing. This served to familiarize the test animals with the apparatus and to reduce novelty-related locomotor hyperactivity, which may potentially confound social interaction during the critical test phase. The rectangular wire cages (located at the end of two arms) were left empty during the habituation phase. During habituation, each test mouse was gently placed in the start arm and allowed to explore the apparatus for 5 min.

The test phase took place one day after the habituation day. During the test phase, one metal wire cage contained an unfamiliar C57BL6/N mouse of the same sex (12–14 weeks of age), whereas the other wire cage contained an inanimate dummy object. The latter was a black scrunchie made of velvet material. The allocation of the unfamiliar live mouse and inanimate dummy object to the two wire cages was counterbalanced across experimental groups. To start a test trial, the test mouse was gently placed in the start arm and allowed to explore freely for 5 min. Behavioral observations were made by an experimenter who was blinded to the experimental conditions, and social interaction was defined as nose contact within a 2-cm interaction zone. For each animal, a social preference index was calculated the by the formula ([time spent with the mouse] / [time spent with the inanimate object + time spent with the mouse]) − 0.5. The social preference index was used to compare the relative exploration time between the unfamiliar mouse and the inanimate dummy object, with values >0 signifying a preference towards the unfamiliar mouse. In addition to the analysis of social interaction scores, the total distance moved was recorded and analyzed to assess general activity. This was achieved by a digital camera mounted above the apparatus, which captured images at a rate of 5 Hz. The images were transmitted to a PC running the EthoVision tracking system (Noldus Information Technology), which provided the measure of the total distance moved (m) during the 5-min testing period. For each animal, the social preference index and total distance moved were included as continuous variables in the cluster analysis (see below).

2.4.2. PPI of the acoustic startle reflex

PPI of the acoustic startle reflex refers to the reduction in startle reaction in response to a startle-eliciting pulse stimulus when it is shortly preceded by a weak prepulse stimulus. The apparatus consisted of four startle chambers for mice (San Diego Instruments, San Diego, CA, USA) and has been fully described elsewhere (Weber-Stadlbauer et al., 2017; Mueller et al., 2021). In the demonstration of PPI, the animals were presented with a series of discrete trials comprising a mixture of four trial types. These included pulse-alone trials, prepulse-plus-pulse trials, prepulse-alone trials, and no-stimulus trials in which no discrete stimulus other than the constant background noise was presented. The pulse and prepulse stimuli used were in the form of a sudden elevation in broadband white noise level (sustaining for 40 and 20 ms, respectively) from the background (65 dBA), with a rise time of 0.2–1.0 ms. In all trials, three different intensities of pulse (100, 110, and 120 dBA) and three intensities of prepulse (71, 77, and 83 dBA, which corresponded to +6, +12, and +18 dBA above background, respectively) were used. The stimulus-onset asynchrony of the prepulse and pulse stimuli on all prepulse-plus-pulse trials was 100 ms (onset-to-onset).

The protocol used for the PPI test was extensively validated before (Weber-Stadlbauer et al., 2017; Mueller et al., 2021). A session began with the animals being placed into the Plexiglas enclosure. They were acclimatized to the apparatus for 2 min before the first trial began. The first 6 trials consisted of 6 startle- alone trials; such trials served to habituate and stabilize the animals' startle response and were not included in the analysis. Subsequently, the animals were presented with 10 blocks of discrete test trials. Each block consisted of the following: three pulse-alone trials (100, 110, or 120 dBA), 3 prepulse-alone trials (+6, +12, or +18 dBA above background), 9 possible combinations of prepulse-plus-pulse trials (3 levels of pulse × 3 levels of prepulse), and one no stimulus trial. The 16 discrete trials within each block were presented in a pseudorandom order, with a variable interval of 15 s on average (ranging from 10 to 20 s). For each of the 3 pulse intensities (100, 110, or 120 dBA), PPI was indexed by percent inhibition of the startle response obtained in the pulse-alone trials by the following expression: 100 % × [1−(mean reactivity on prepulse-plus-pulse trials/mean reactivity on pulse-alone trials)], for each animal, and at each of the three possible prepulse intensities (+6, +12, or +18 dBA above background). In addition to PPI, reactivity to pulse-alone trials were also analyzed. For each animal, the mean % PPI (average % PPI across all prepulse and pulse conditions) and the mean pulse reactivity (pulse reactivity across all pulse conditions) were included as continuous variables in the cluster analysis (see below).

2.5. Collection of adult brain samples

One week after behavioral testing, CON and MIA offspring were killed by decapitation using surgical scissors without prior anesthesia. The brains were rapidly extracted from the skull (within <30 s), immediately frozen on powdered dry ice and kept at −80 °C until further processing. Frozen coronal sections were then prepared using razorblade cuts in order to collect micropunches of the medial prefrontal cortex (mPFC, including anterior cingulate, prelimbic and dorsal parts of the infralimbic cortices; bregma: +2.3 to +1.3 mm). The mPFC punches were then immediately processed further for RNA extraction (see below). The mPFC was selected for two main reasons. First, it represents a cortical brain area with broad relevance for neurodevelopmental disorders (Schubert et al., 2015). Second, the mPFC displays distinct transcriptional profiles in offspring developing behavioral deficits after MIA as compared to MIA-exposed offspring showing no behavioral deficits (Mueller et al., 2021).

2.6. RNA extraction and quantitative real-time PCR analyses

RNA extraction and quantitative real-time PCR analyses were performed according to previously established protocols (Labouesse et al., 2018; Notter et al., 2021). In brief, total RNA was isolated from placental samples, fetal brains and adult mPFC samples using the SPLIT RNA Extraction Kit (008.48, Lexogen, Vienna, Austria). The procedure was conducted according to the manufacturer's instructions, and the resulting RNA was quantified by Nanodrop (DeNovix DS-11+ spectrophotometer, Labgene Scientific SA, Switzerland). RNA was reverse-transcribed into cDNA using iScript™ cDNA Synthesis Kit (Biorad, Hercules, California, USA) according to the manufacturer's instructions, and the samples were stored at −80 °C until further use.

The Biorad CFX384™ Real-Time System (Biorad, Hercules, California, USA) using SYBR Green SsoAdvanced™ Universal SYBR® Green Supermix (Biorad, Hercules, California, USA) was used for quantitative real-time PCR to measure the mRNA levels of seven murine ERVs (ETnI, ETnIIα, ETnIIβ, IAP, MusD, SynA, and SynB) and IL-6. All primers were purchased from Eurofins Genomics GmbH (Germany). The samples were run in 384-well formats in triplicates as multiplexed reactions with a normalizing internal control (glyceraldehyde 3-phosphate dehydrogenase, GAPDH). The real-time PCR reaction included 2.5 ng cDNA, 150 nM forward and reverse primers for each ERV gene, 300 nM for IL-6, and 2.5 μl of SsoAdvanced™ Universal SYBR® Green Supermix (Biorad, Hercules, California, USA) in a total volume of 5 μl. Thermal cycling was initiated at 95 °C for 30 s, followed by 40 PCR cycles (10 s at 95 °C; 20 s at 60 °C), and a melt-curve analysis (65–95 °C, 0.5 °C increments at 5 *sec*/step). Each sample was analysed in triplicate and a negative control (no template reaction) was included in each experiment to rule out any possible contamination. Relative target gene expression was calculated according to the $2^{-\Delta\Delta Ct}$ method (Livak and Schmittgen, 2001). Probe and primer sequences of each gene of interest were validated in previous studies (Baust et al., 2003; Cipriani et al., 2018b) and are summarized in Table 1.

2.7. Quantification of IL-6 protein in maternal plasma

Protein levels of IL-6 were quantified in maternal plasma samples using a *meso*-Scale Discovery (MSD) electrochemoluminescence assay (MSD, Rockville, Maryland, USA) for mice as previously described (Mueller et al., 2019; 2021). The plates were read using the SECTOR PR 400 (MSD) imager and analyzed using MSD's Discovery Workbench analyzer and software package (Mueller et al., 2019; 2021). All assays were run in duplicates according to the manufacturer's instructions. The detection limit of IL-6 was 0.63 pg/ml.

2.8. Statistical analyses

All statistical analyses were performed using SPSS Statistics (version 25.0, IBM, Armonk, NY, USA) and Prism (version 8.0; GraphPad Software, La Jolla, California), with statistical significance set at $p < 0.05$. Unless specified otherwise, all data were analyzed separately for male and female offspring. Gene expression data from placental and fetal brain samples were analyzed using independent Student's *t* tests (two-tailed). Correlations between maternal IL-6 levels and placental or fetal gene transcripts, and between fetal and placental gene transcripts, were conducted using first-order partial correlations, thereby applying Bonferroni correction to protect the data against type I errors resulting from multiple comparisons.

To identify subgroups of MIA-exposed offspring based on behavioral performances in adulthood, the main behavioral readouts (social preference index and total distance moved in the social interaction test; mean % PPI and mean pulse reactivity in the PPI test) were analyzed by two-step cluster analyses, as described before (Mueller et al., 2021). In brief, the behavioral readouts from each individual CON and MIA offspring were fed into the cluster analysis without predetermining the number of clusters, thereby avoiding bias in terms of identifying cluster numbers. The Bayesian information criterion was used to estimate the maximum number of clusters, and the log-likelihood method was used as the distance measure (Mueller et al., 2021). Following stratification of MIA offspring into Sus-MIA and Res-MIA subgroups by two-step cluster analysis, one-way analysis of variance (ANOVA) and Tukey's post-hoc test for multiple comparisons were used to compare the behavioral scores between MIA subgroups and CON offspring. The same subgroup identities were then used to compare the mRNA levels of IL-6 and ERVs between Sus-MIA and Res-MIA relative to CON offspring using one-way ANOVA, followed by Tukey's post-hoc test for multiple comparisons whenever appropriate. Possible correlations between IL and 6 and ERV mRNA levels in adult mPFC samples were conducted using first-order partial correlations, thereby applying Bonferroni correction to protect the data against type I errors resulting from multiple comparisons. Likewise, Bonferroni-corrected first-order partial correlations were used to assess possible correlations between behavioral data and ERV mRNA levels in adult mPFC samples.

Table 1
List of forward and reverse primer sequences used in this study.

Gene	Forward primer sequence	Reverse primer sequence
ETnI	5′- GTTAAACCCGAGCGCTGGTTC-3′	5′-GCTATAAGGCCCAGAGAGAAATTTC-3′
ETnIIα	5′- CCAGC(C/T)(A/C)TTCTAACTCAATC-3′	5′- GCAGGGAGTAATCTATGTAAG-3‘
ETnIIβ	5′- CCAGC(C/T)(A/C)TTCTAACTCAATC-3′	5′-CATT(T/C)(G/A)TTAGT(C/T)AGGGGGTATTAAGTGAC-3‘
GAPDH	5′-AACGACCCCTTCATTGAC-3′	5′-CTCCACGACATACTCAGCAC-3′
IAP	5′-AAGCAGCAATCACCCACTTTGG-3′	5′-CAATCATTAGATG(T/C)GGCTGCCAAG-3′
IL-6	5′-GTTCTCTGGGAAATCGTGGA-3′	5′-TGTACTCCAGGTAGCTATGG-3′
MusD	5′-GATTGGTGGAAGTTTAGCTAGCAT-3′	5′-TAGCATTCTCATAAGCCAATTGCAT-3′
SynA	5′-CATCTATGCTGGATGAAGCCT-3′	5′-AGACCCTGGCATGGCCATTA-3′
SynB	5′-GCCCGTTGATCTCAGCCTCCT-3′	5′-GGCATCCGGTCTTTTCATTGC-3′

The list specifies forward and reverse primer sequences used for quantifying endogenous retroviral elements (ETnI, ETnIIα, ETnIIβ, IAP, MusD, SynA, and SynB), IL-6, and the reference gene (GAPDH). All probe and primer sequences were validated in previous studies (Baust et al., 2003; Cipriani et al., 2018b).

3. Results

3.1. Effects of MIA on the expression of ERVs in the placenta

First, we investigated the post-acute effects of MIA on IL-6 and ERV expression in placental samples of male and female offspring. As expected (Hsiao and Patterson, 2011; Mueller et al., 2019), MIA increased placental IL-6 mRNA levels in male ($t_{(8)} = 5.7$, $p = 0.0004$; Fig. 1b) and female ($t_{(8)} = 5.1$, $p = 0.0009$; Fig. 1e) offspring. In both sexes, MIA also upregulated the expression of placental ETnI (male placentae: $t_{(8)} = 2.4$, $p = 0.045$, Fig. 1a; female placentae: $t_{(8)} = 2.5$, $p = 0.036$, Fig. 1d) and ETnIIα (male placentae: $t_{(8)} = 2.5$, $p = 0.044$, Fig. 1a; female placentae: $t_{(8)} = 3.8$, $p = 0.006$, Fig. 1d), whereas placental ETnIIβ expression was only increased in female ($t_{(8)} = 3.0$, $p = 0.017$; Fig. 1d) but not in male (Fig. 1a) offspring of MIA-exposed dams. On the other hand, MIA decreased placental expression of IAP, SynA and SynB in both male (IAP: $t_{(8)} = 2.7$, $p = 0.028$; SynA: $t_{(8)} = 2.4$, $p = 0.042$; SynB: $t_{(8)} = 2.8$, $p = 0.027$; Fig. 1a) and female (IAP: $t_{(8)} = 2.8$, $p = 0.031$; SynA: $t_{(8)} = 6.8$, $p = 0.0005$; SynB: $t_{(8)} = 5.1$, $p = 0.001$; Fig. 1d) offspring. In placentae of male offspring, IL-6 mRNA levels correlated positively with ETnI and negatively with SynB mRNA levels (Fig. 1c), whereas IL-6 mRNA levels correlated positively with ETnIIα and negatively with SynA and SynB mRNA levels in placentae of female offspring (Fig. 1f).

3.2. Effects of MIA on the expression of ERVs in the fetal brain

We then assessed the post-acute effects of MIA on IL-6 and ERV expression in the fetal brains of male and female offspring. Consistent with the effects observed in placental tissues (Fig. 1), MIA increased IL-6 mRNA levels in male ($t_{(8)} = 3.2$, $p = 0.009$; Fig. 2b) and female ($t_{(8)} = 2.4$, $p = 0.045$; Fig. 2e) fetal brains. MIA also upregulated the expression of ETnI in the fetal brains of male ($t_{(8)} = 2.6$, $p = 0.041$; Fig. 2a) but not female (Fig. 2d) offspring. Furthermore, there was a marked sex-specific effect of MIA on the expression of SynB in fetal brains, which was found to be reduced in males ($t_{(8)} = 3.8$, $p = 0.006$; Fig. 2a) but increased in females ($t_{(8)} = 2.4$, $p = 0.045$; Fig. 2d). In addition, MusD mRNA levels were reduced in the fetal brains of male ($t_{(8)} = 2.3$, $p = 0.048$; Fig. 2a) but not female (Fig. 2d) offspring exposed to MIA. In fetal brains of male offspring, IL-6 mRNA levels correlated negatively with SynB mRNA levels (Fig. 2c), whereas there was a positive correlation between these two genes in the fetal brains of female offspring (Fig. 2e).

3.3. Relationship between maternal IL-6 levels and placental and fetal gene transcripts

To identify possible relationships between maternal IL-6 levels and placental and fetal gene transcripts, we quantified IL-6 protein in maternal plasma for subsequent correlations with mRNA levels of IL-6 and ERVS in placental (Fig. 1) and fetal (Fig. 2) tissues. As expected (Mueller et al., 2019; 2021), MIA led to a marked elevation of IL-6 in maternal plasma ($t_{(8)} = 7.8$, $p = 0.0001$; Fig. 3a). Maternal IL-6 levels correlated positively with the levels of IL-6 and ETnI transcripts in the placentae of male offspring, whereas it correlated negatively with placental SynB transcripts in males (Fig. 3b). Furthermore, maternal IL-6 correlated positively and negatively with the transcript of IL-6 and SynB, respectively, in the fetal brains of male offspring (Fig. 3b). In female offspring, there were positive correlations between maternal IL-6 levels and placental IL-6, ETnI, ETnIIα, and ETnIIβ transcripts, whereas maternal IL-6 correlated negatively with placental SynA and SynB transcripts (Fig. 3c). None of the correlations attained statistical significance in the fetal brains of female offspring (Fig. 3c).

3.4. Stratification of MIA-exposed offspring into resilient and susceptible subgroups based on adult behavioral profiles

We have previously shown that offspring of MIA-exposed mothers can be stratified into subgroups that are characterized by the presence (susceptible subgroup) or absence (resilient subgroup) of overt behavioral anomalies at adult age (Mueller et al., 2021). The identification of such subgroups provides an opportunity to explore whether resilience and susceptibility to MIA is associated with differential expression of ERVs. Therefore, we generated a cohort of CON and MIA offspring and stratified them into resilient and susceptible subgroups based on their behavioral performance in the social interaction and PPI tests conducted at adult age. The values of the main behavioral readouts corresponding to each individual CON and MIA animal are depicted in Suppl. Fig. S1.

In male offspring, two-step cluster analysis identified two main clusters (CL1 and CL2), which contained 70.8 % (CL1) and 29.2 % (CL2) of all males (Fig. 4a). The social preference index obtained from the social interaction test had the highest predictor importance for cluster separation in males, followed by the mean % PPI scores (Fig. 4a). As shown in Fig. 4b, 56.3 % ($N = 9$) and 43.7 % ($N = 7$) of male MIA offspring were assigned to CL1 and CL2, respectively, whereas all ($N = 8$) male CON offspring were classified as belonging to CL1. Overall, male offspring from CL2 were characterized by a lower social preference index and lower PPI scores as compared to CL1 offspring. Therefore, MIA offspring in CL1 were referred to as resilient (Res-MIA subgroup), whereas MIA offspring in CL2 were classified as susceptible (Sus-MIA subgroup). The subsequent comparison of CON, Res-MIA and Sus-MIA subgroups confirmed that male Sus-MIA, but not male Res-MIA offspring, displayed a significantly reduced social preference index compared to male CON offspring (ANOVA: $F_{(2,21)} = 28.3$, $p = 0.0001$; Sus-MIA vs CON: $p = 0.0001$; Sus-MIA vs Res-MIA: $p = 0.0002$; Fig. 4c). Likewise, only male Sus-MIA, but not male Res-MIA offspring, displayed a significant decrease in mean% PPI as compared to male CON offspring (ANOVA: $F_{(2,21)} = 12.1$, $p = 0.0003$; Sus-MIA vs CON: $p = 0.0007$; Sus-MIA vs Res-MIA: $p = 0.0009$; Fig. 4d). There were no significant differences between subgroups in terms of the total distance moved in the social interaction test (Fig. 4c) or mean pulse reactivity in the PPI test (Fig. 4d).

A similar stratification into resilient and susceptible subgroups was also obtained in female offspring of MIA-exposed mothers. Two-step

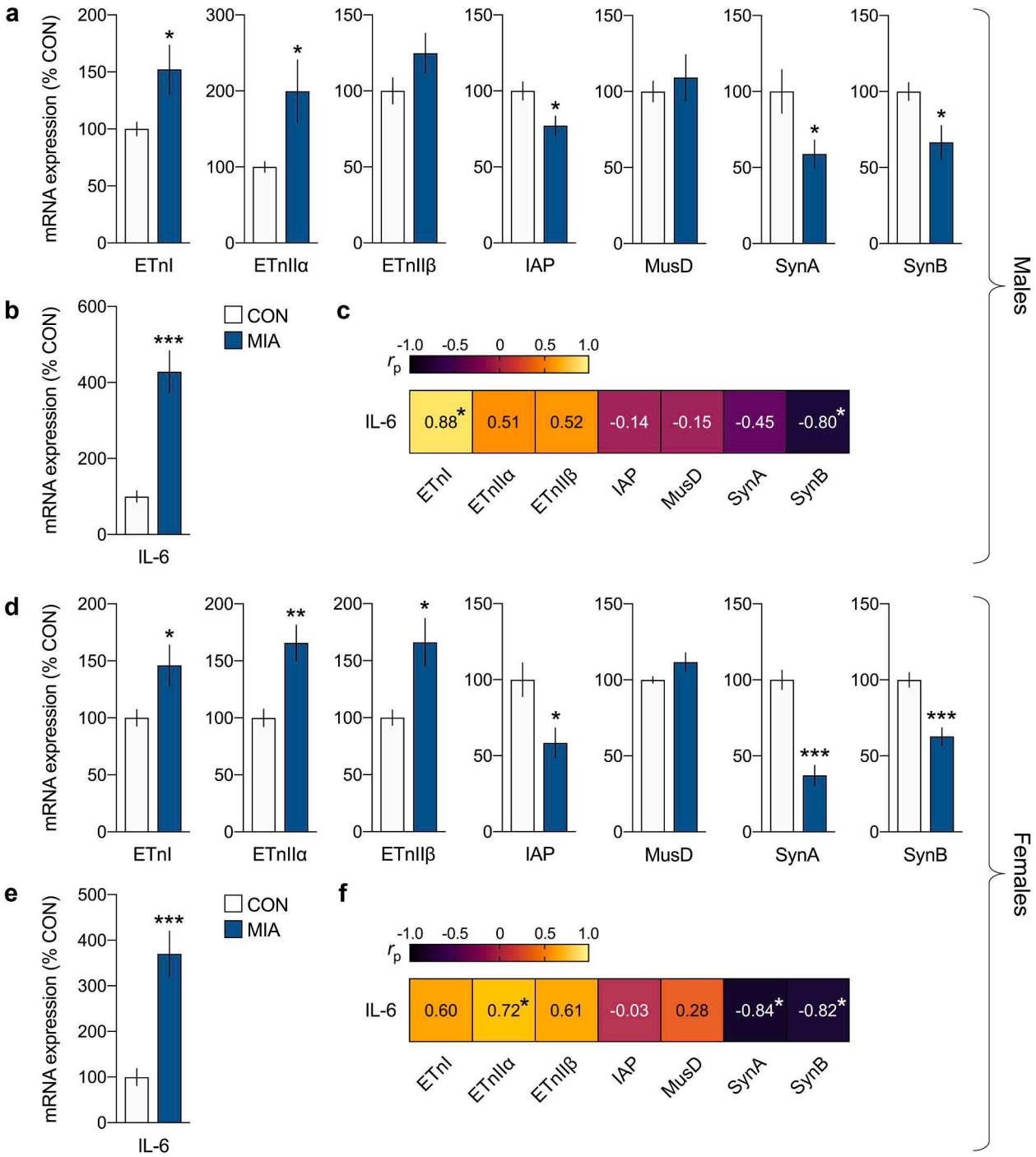

Fig. 1. Effects of MIA on the expression of endogenous retroviral elements in the placenta. Quantitative real-time PCR analyses were performed using placental samples obtained from control (CON) or MIA-exposed dams. Each gene of interest is depicted as mRNA expression relative to CON (% CON). **(a)** Expression of endogenous retroviral elements in placental samples of male fetuses. **(b)** Expression of IL-6 in placental samples of male fetuses. **(c)** Partial correlations between IL-6 and endogenous retroviral elements in placental samples of male fetuses. Negative and positive correlations are represented in dark purple and yellow color, respectively. Significant correlations are denoted with the symbol (*), thereby correcting the data for multiple comparisons (significance threshold: $^*p < 0.0071$). **(d)** Expression of endogenous retroviral elements in placental samples of female fetuses. **(e)** Expression of IL-6 in placental samples of female fetuses. **(f)** Partial correlations between IL-6 and endogenous retroviral elements in placental samples of female fetuses. Negative and positive correlations are represented in dark purple and yellow color, respectively. Significant correlations are denoted with the symbol (*), thereby correcting the data for multiple comparisons (significance threshold: $^*p < 0.0071$). All gene expression values represent means ± SEM; $^*p < 0.05$, $^{**}p < 0.01$ and $^{***}p < 0.001$, based on independent *t*-tests (two-tailed); N[CON] = 5 per sex, N[MIA] = 5 per sex.

cluster analysis identified two main clusters (CL1 and CL2), which contained 62.5 % (CL1) and 37.5 % (CL2) of all female offspring (Fig. 4e). Like in male offspring, the social preference index had the highest predictor importance for cluster separation in females, followed by the mean % PPI scores (Fig. 4e). As shown in Fig. 4f, 43.7 % ($N = 7$) and 56.3 % ($N = 9$) of female MIA offspring were assigned to CL1 and CL2, respectively, whereas all ($N = 8$) female CON offspring were classified as belonging to CL1. Consistent with males, female MIA

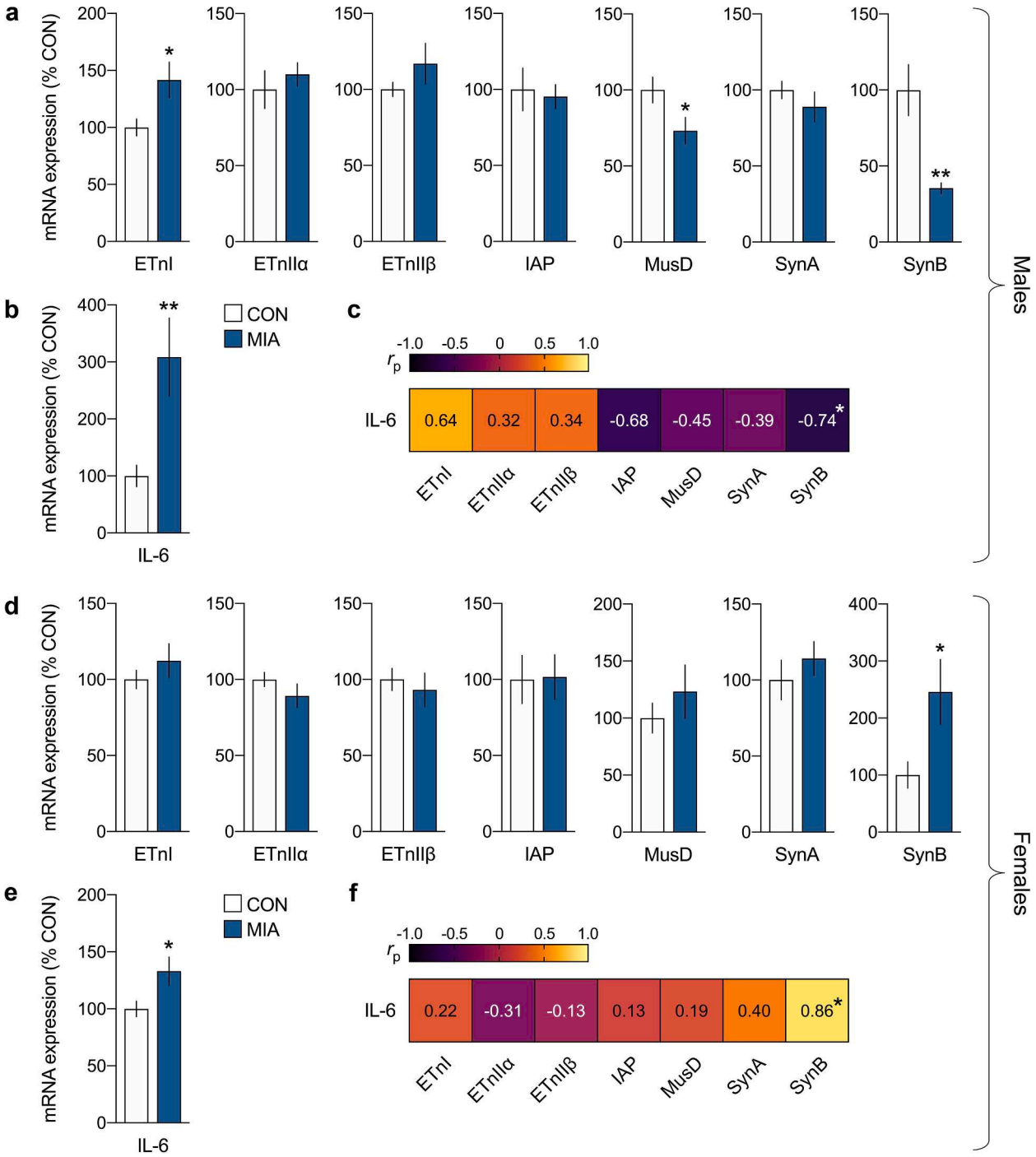

Fig. 2. Effects of MIA on the expression of endogenous retroviral elements in the fetal brain. Quantitative real-time PCR analyses were performed using fetal brain samples obtained from control (CON) or MIA-exposed dams. Each gene of interest is depicted as mRNA expression relative to CON (% CON). **(a)** Expression of endogenous retroviral elements in male fetal brains. **(b)** Expression of IL-6 in male fetal brains. **(c)** Partial correlations between IL-6 and endogenous retroviral elements in male fetal brains. Negative and positive correlations are represented in dark purple and yellow color, respectively. Significant correlations are denoted with the symbol (*), thereby correcting the data for multiple comparisons (significance threshold: $^*p < 0.0071$). **(d)** Expression of endogenous retroviral elements in female fetal brains. **(e)** Expression of IL-6 in female fetal brains. **(f)** Partial correlations between IL-6 and endogenous retroviral elements in female fetal brains. Negative and positive correlations are represented in dark purple and yellow color, respectively. Significant correlations are denoted with the symbol (*), thereby correcting the data for multiple comparisons (significance threshold: $^*p < 0.0071$). All gene expression values represent means ± SEM; $^*p < 0.05$, $^{**}p < 0.01$ and $^{***}p < 0.001$, based on independent *t*-tests (two-tailed); *N*[CON] = 5 per sex, *N*[MIA] = 5 per sex.

offspring from CL2 (Sus-MIA subgroup) were characterized by a lower social preference index and lower PPI scores as compared to female MIA offspring from CL1 (Res-MIA subgroup). The comparison of CON, Res-MIA and Sus-MIA subgroups confirmed that female Sus-MIA, but not female Res-MIA offspring, displayed a significantly reduced social preference index compared to female CON offspring (ANOVA: $F_{(2,21)} = 36.9$, $p = 0.0002$**;** Sus-MIA vs CON: $p = 0.0001$; Sus-MIA vs Res-MIA: $p = 0.0002$; Fig. 4g). Likewise, only female Sus-MIA, but not female Res-MIA offspring, showed a significant decrease in mean% PPI as compared to female CON offspring (ANOVA: $F_{(2,21)} = 7.2$, $p = 0.004$; Sus-MIA vs

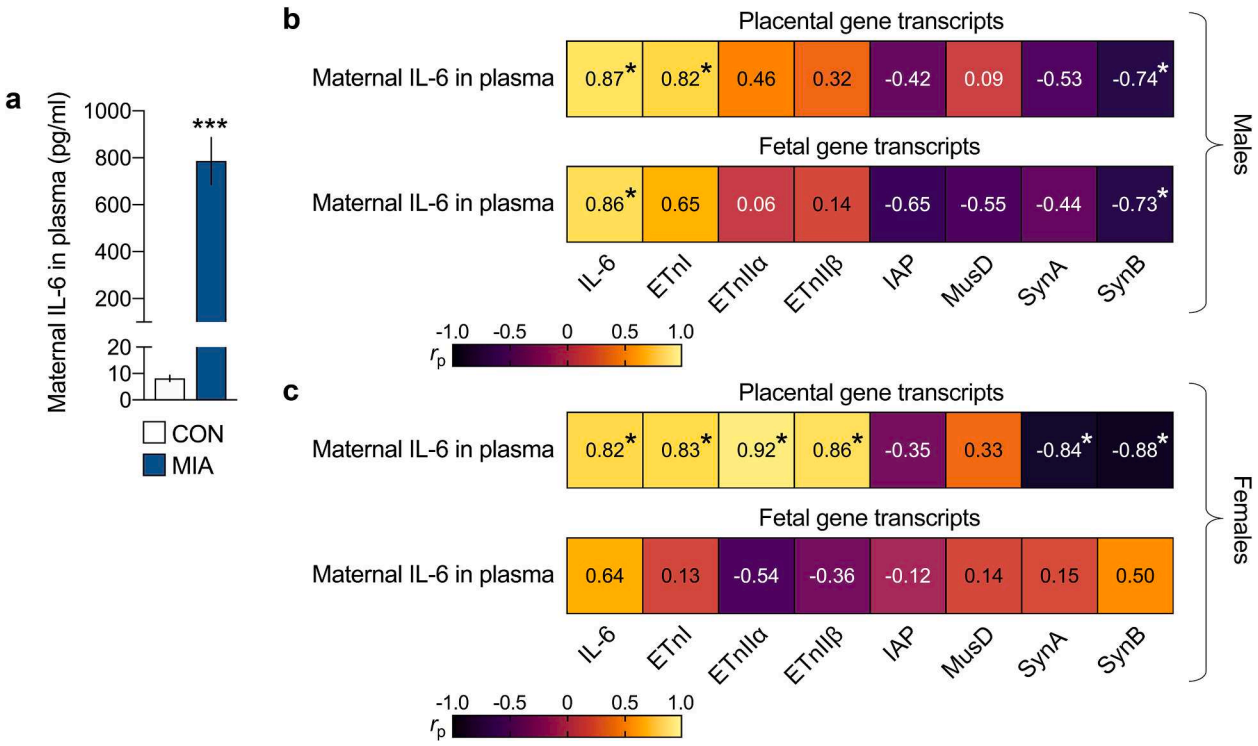

Fig. 3. Relationship between maternal IL-6 levels and placental and fetal gene transcripts. **(a)** IL-6 protein levels (means ± SEM) in maternal plasma 6 hrs after control (CON) treatment or poly(I:C)-induced maternal immune activation (MIA). N[CON] = 5 dams, N[MIA] = 5 dams. ***$p < 0.001$, based on independent t-test (two-tailed). **(b)** Partial correlations between maternal IL-6 levels in plasma and gene transcripts (IL-6, ETnI, ETnIIα, ETnIIβ, IAP, MusD, SynA, and SynB) in the placentae and fetal brains of male offspring. Negative and positive correlations are represented in dark purple and yellow color, respectively. Significant correlations are denoted with the symbol (*), thereby correcting the data for multiple comparisons (significance threshold: *$p < 0.0063$). N[CON] = 5 and N[MIA] = 5, originating from 5 independent litters each. **(c)** Partial correlations between maternal IL-6 levels in plasma and gene transcripts (IL-6, ETnI, ETnIIα, ETnIIβ, IAP, MusD, SynA, and SynB) in the placentae and fetal brains of female offspring. Negative and positive correlations are represented in dark purple and yellow color, respectively. Significant correlations are denoted with the symbol (*), thereby correcting the data for multiple comparisons (significance threshold: *$p < 0.0063$). N[CON] = 5 and N[MIA] = 5, originating from 5 independent litters each.

CON: $p = 0.015$; Sus-MIA vs Res-MIA: $p = 0.006$; Fig. 4h). There were no significant differences between female subgroups in terms of the total distance moved in the social interaction test (Fig. 4g) or mean pulse reactivity in the PPI test (Fig. 4h).

In an additional cluster analysis, we combined the behavioral data from male and female offspring to explore whether the stratification of MIA offspring into Sus-MIA and Res-MIA subgroups would be comparable to the analyses that were split by sex. As summarized in Suppl. Fig. S2, we found that the relative number of Sus-MIA and Res-MIA offspring remained the same as when the cluster analyses were conducted for each sex separately (Fig. 4). Consistent with the analyses split by sex (Fig. 4), the social preference index had the highest predictor importance for cluster separation in the combined cluster analysis, followed by the mean % PPI scores (Suppl. Fig. S2). As shown in Suppl. Fig. S3, contrasting between- and within-litter effects demonstrated that Sus-MIA and Res-MIA offspring were distributed relatively evenly across all MIA-exposed litters. Hence, each MIA litter concomitantly contained Sus-MIA and Res-MIA offspring, indicating that the stratification of the two subgroups is mainly driven by within-litter rather than between-litter variability.

3.5. *Expression of ERVs in resilient and susceptible subgroups of MIA-exposed offspring*

The presence of subgroups of MIA-exposed offspring with or without overt behavioral anomalies provides a unique opportunity to examine whether ERVs may be differentially expressed in the brains of resilient and susceptible offspring. Therefore, we compared the transcripts of ERVs in the mPFC of CON, Res-MIA and Sus-MIA offspring that were behaviorally characterized and stratified based on dissociable behavioral profiles (Fig. 4).

As shown in Fig. 5a, male Sus-MIA offspring displayed a consistent increase in the expression of ERVs relative to male CON and/or Res-MIA offspring, with significant effects obtained for ETnI (ANOVA: $F_{(2,21)} = 7.3$, $p = 0.005$; Sus-MIA vs CON: $p = 0.028$; Sus-MIA vs Res-MIA: $p = 0.007$), ETnIIα (ANOVA: $F_{(2,21)} = 7.5$, $p = 0.004$; Sus-MIA vs CON: $p = 0.041$; Sus-MIA vs Res-MIA: $p = 0.003$), ETnIIβ (ANOVA: $F_{(2,21)} = 6.1$, $p = 0.009$; Sus-MIA vs Res-MIA: $p = 0.007$), IAP (ANOVA: $F_{(2,21)} = 9.7$, $p = 0.001$; Sus-MIA vs CON: $p = 0.016$; Sus-MIA vs Res-MIA: $p = 0.0008$), MusD (ANOVA: $F_{(2,21)} = 7.1$, $p = 0.004$; Sus-MIA vs CON: $p = 0.042$; Sus-MIA vs Res-MIA: $p = 0.003$), SynA (ANOVA: $F_{(2,21)} = 8.3$, $p = 0.004$; Sus-MIA vs Res-MIA: $p = 0.003$), and SynB (ANOVA: $F_{(2,21)} = 4.8$, $p = 0.031$; Sus-MIA vs CON: $p = 0.026$). Likewise, the levels of IL-6 mRNA were selectively increased in the mPFC of male Sus-MIA offspring (ANOVA: $F_{(2,21)} = 21.7$, $p = 0.0001$; Sus-MIA vs CON: $p = 0.0003$; Sus-MIA vs Res-MIA: $p = 0.0004$ Fig. 5b). By contrast, male Res-MIA offspring did not differ from male CON offspring with regards to the expression of ERVs (Fig. 5a) or IL-6 (Fig. 5b). Partial correlations further demonstrated that IL-6 mRNA levels in the mPFC of male offspring correlated positively with ETnI, IAP, SynA, and SynB mRNA levels (Fig. 5c).

Consistent with males, female Sus-MIA offspring displayed an increase in the mRNA levels of SynB (ANOVA: $F_{(2,21)} = 7.9$, $p = 0.005$; Sus-MIA vs CON: $p = 0.032$; Sus-MIA vs Res-MIA: $p = 0.005$; Fig. 5d) and IL-6 (ANOVA: $F_{(2,21)} = 7.5$, $p = 0.006$; Sus-MIA vs CON: $p = 0.013$; Sus-MIA vs Res-MIA: $p = 0.007$; Fig. 5e) as compared to female CON and/or Res-MIA offspring. In contrast to male offspring, however, the transcripts of all other ERVs were consistently reduced in female Res-MIA offspring as compared to CON and/or Sus-MIA offspring (Fig. 5d), with significant

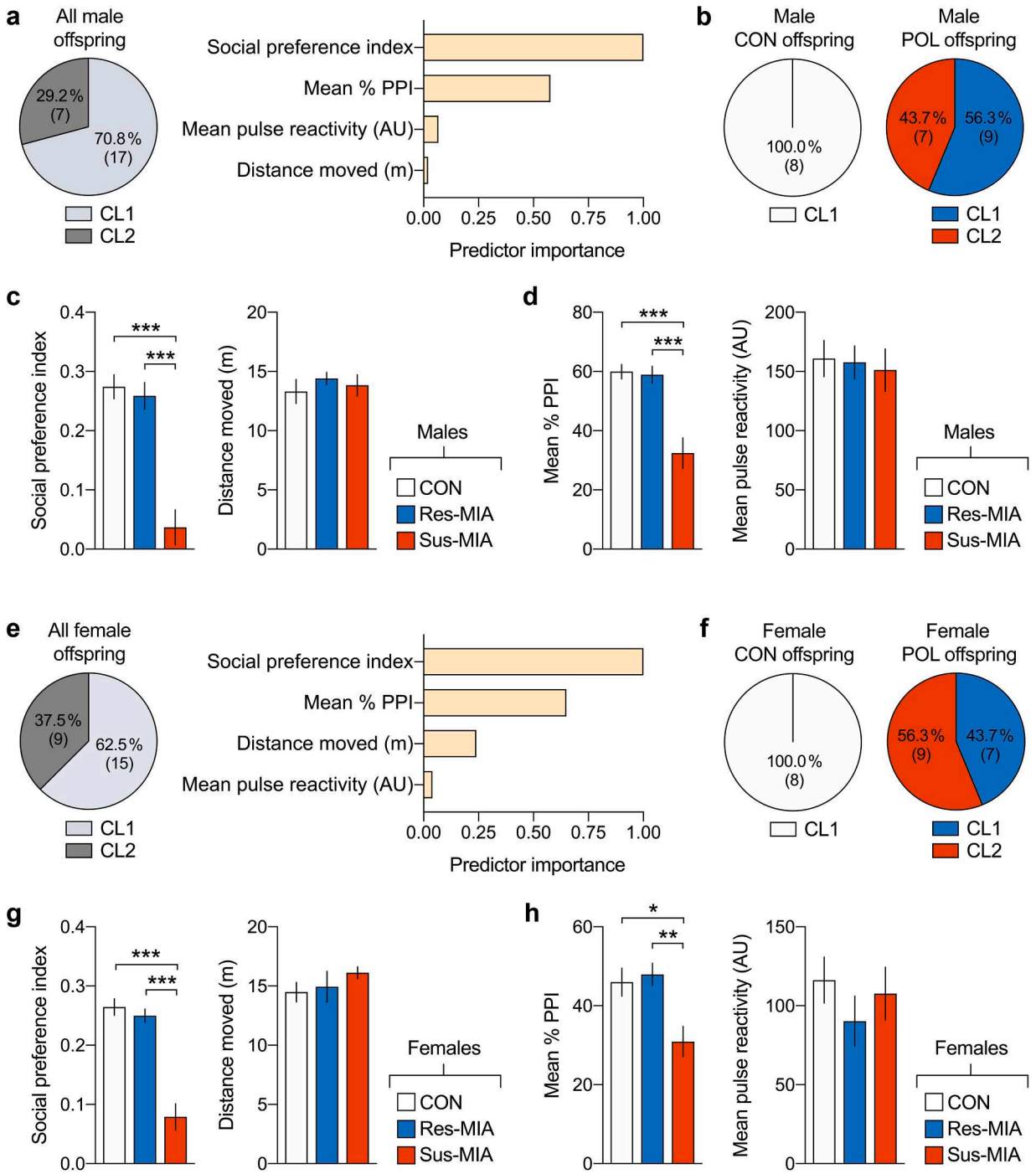

Fig. 4. Stratification of MIA-exposed offspring into resilient and susceptible subgroups. A two-step cluster analysis incorporating the main behavioral measures (social preference index and distance moved in the social interaction test; mean % PPI and mean pulse reactivity in the PPI test) was performed to identify subgroups with differing behavioral profiles. **(a)** Distribution of all male offspring across the two clusters (CL1 and CL2) identified by two-step cluster analysis. The pie chart shows the cluster distribution (in percentages, %) for all male offspring combined, with numbers in brackets representing the number of male offspring in each cluster. The bar plot depicts the relative predictor importance for cluster separation in male offspring. **(b)** Distribution of male CON and MIA offspring across the two clusters (CL1 and CL2). The numbers in brackets represent the number of male CON and MIA offspring in each cluster. **(c)** Social preference index and distance moved in the social interaction test for male CON offspring, resilient MIA offspring (Res-MIA) and susceptible MIA offspring (Sus-MIA). **(d)** Mean % PPI scores and mean pulse reactivity (in arbitrary units, AU) for male CON, Res-MIA and Sus-MIA offspring. **(e)** Distribution of all female offspring across the two clusters (CL1 and CL2) identified by two-step cluster analysis. The pie chart shows the cluster distribution (in percentages, %) for all female offspring combined, with numbers in brackets representing the number of female offspring in each cluster. The bar plot depicts the relative predictor importance for cluster separation in female offspring. **(f)** Distribution of female CON and MIA offspring across the two clusters (CL1 and CL2). The numbers in brackets represent the number of female CON and MIA offspring in each cluster. **(g)** Social preference index and distance moved in the social interaction test for female CON, Res-MIA and Sus-MIA offspring. **(h)** Mean % PPI scores and mean pulse reactivity (in arbitrary units, AU) for female CON, Res-MIA and Sus-MIA offspring. All values represent means ± SEM; $*p < 0.05$, $**p < 0.01$ and $***p < 0.001$, based on Tukey's post-hoc test for multiple comparisons after ANOVA.

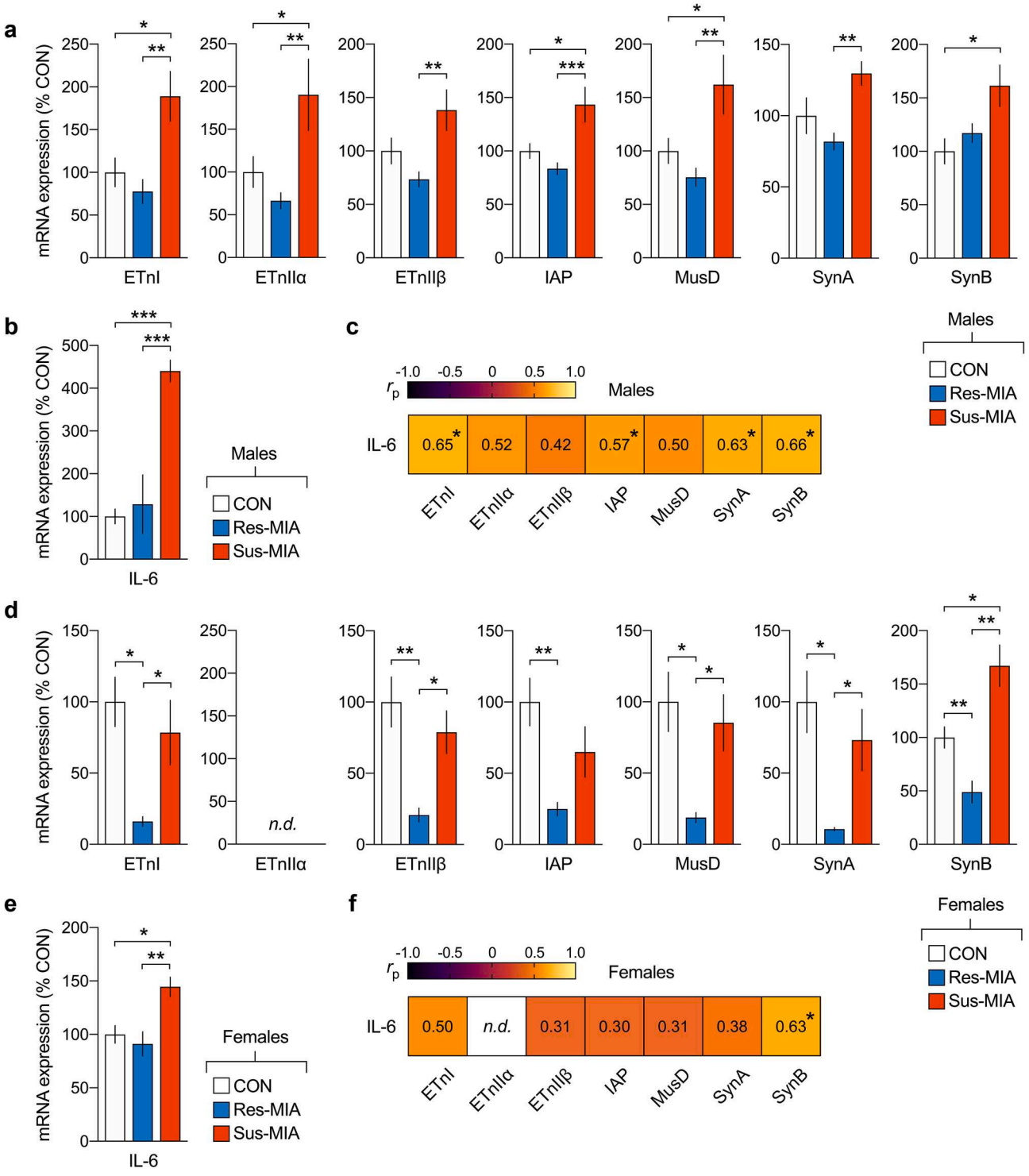

Fig. 5. Expression of endogenous retroviral elements and IL-6 in adult control offspring and subgroups of MIA-exposed offspring. Quantitative real-time PCR analyses were performed using mPFC samples from adult CON offspring, resilient MIA offspring (Res-MIA) and susceptible MIA offspring (Sus-MIA), which were stratified based on their behavioral performance (see Fig. 4). Each gene of interest is depicted as mRNA expression relative to CON (% CON). **(a)** Expression of endogenous retroviral elements in male offspring. **(b)** Expression of IL-6 in male offspring. **(c)** Partial correlations between IL-6 and endogenous retroviral elements in male offspring. Negative and positive correlations are represented in dark purple and yellow color, respectively. Significant correlations are denoted with the symbol (*), thereby correcting the data for multiple comparisons (significance threshold: $^*p < 0.0071$). **(d)** Expression of endogenous retroviral elements in female offspring; n.d., not determinable. **(e)** Expression of IL-6 in female offspring. **(f)** Partial correlations between IL-6 and endogenous retroviral elements in male offspring. Negative and positive correlations are represented in dark purple and yellow color, respectively. Significant correlations are denoted with the symbol (*), thereby correcting the data for multiple comparisons (significance threshold: $^*p < 0.0083$). All gene expression values represent means ± SEM; $^*p < 0.05$, $^{**}p < 0.01$ and $^{***}p < 0.001$, based on Tukey's post-hoc test for multiple comparisons after ANOVA.

effects obtained for ETnI (ANOVA: $F_{(2,21)} = 5.2$, $p = 0.016$; Res-MIA vs CON: $p = 0.015$; Res-MIA vs Sus-MIA: $p = 0.041$), ETnIIβ (ANOVA: $F_{(2,21)} = 8.1$, $p = 0.003$; Res-MIA vs CON: $p = 0.002$; Res-MIA vs Sus-MIA: $p = 0.025$), IAP (ANOVA: $F_{(2,21)} = 5.6$, $p = 0.011$; Res-MIA vs CON: $p = 0.008$), MusD (ANOVA: $F_{(2,21)} = 5.9$, $p = 0.009$; Res-MIA vs CON: $p = 0.011$; Res-MIA vs Sus-MIA: $p = 0.038$), and SynA (ANOVA: $F_{(2,21)} = 5.6$, $p = 0.012$; Res-MIA vs CON: $p = 0.011$; Res-MIA vs Sus-MIA: $p = 0.039$). Partial correlations between transcripts of IL-6 and ERVs in female offspring identified a positive correlation between IL-6 and SynB only (Fig. 5f).

3.6. Association between MIA-induced changes in behavior and expression of ERVs

To explore possible associations between the MIA-induced changes in behavior and expression of ERVs in the mPFC of adult offspring, we performed partial correlations between ERV mRNA levels and the primary readouts obtained in the social interaction test (i.e., social preference index) and PPI test (i.e., mean % PPI). In view of the sexually dimorphic expression of ERVs in MIA offspring (Fig. 5), these correlative analyses were performed separately for male and female offspring.

In males, the levels of ERV transcripts correlated inversely with the behavioral scores of interest (Fig. 6a). Following multiple-comparison correction, significant inverse correlations were found between the social preference index and ETnI, ETnIIα or SynB, and between mean % PPI and ETnIIα in male offspring. In females, the inverse correlation between mean % PPI and SynB mRNA levels was the only correlation attaining statistical significance (Fig. 6b).

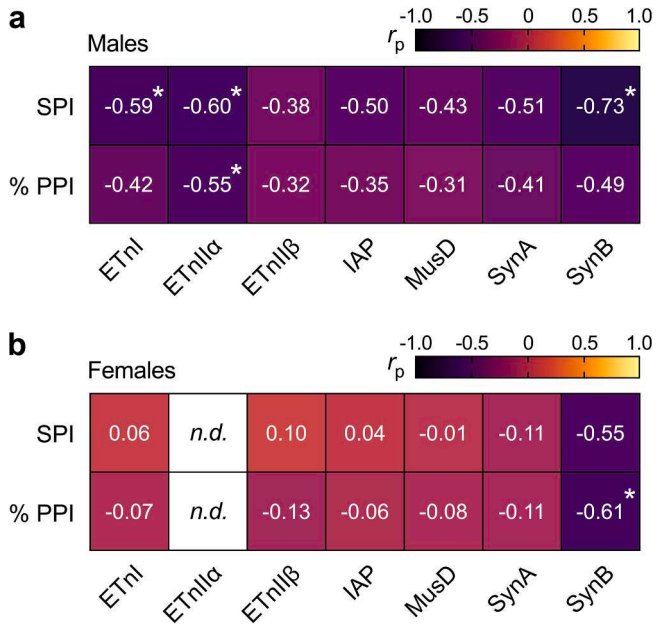

Fig. 6. Correlations between main behavioral readouts and expression of endogenous retroviral elements in adult control offspring and MIA-exposed offspring. The social preference index (SPI) and mean percent prepulse inhibition (% PPI) data used for correlations are summarized in Fig. 4, - whereas gene expression levels of endogenous retroviral elements are summarized in - Fig. 5. All correlations were conducted using partial correlations controlling for prenatal treatment effects. Negative and positive correlations are represented in dark purple and yellow color, respectively. **(a)** Correlations between endogenous retroviral gene expression and SPI or % PPI in male offspring. Significant correlations are denoted with the symbol (*), thereby correcting the data for multiple comparisons (significance threshold: $*p < 0.0071$). **(b)** Correlations between endogenous retroviral gene expression and SPI or % PPI in female offspring. Significant correlations are denoted with the symbol (*), thereby correcting the data for multiple comparisons (significance threshold: $*p < 0.0083$); not determinable.

4. Discussion

Our study identifies short- and long-term changes in the expression of endogenous retroviral elements in the poly(I:C)-based MIA model of neurodevelopmental disorders. The specificity of these changes was dependent on the type of tissue and sex and age of the offspring, as well as on the presence or absence of overt behavioral deficits at adult age. Hence, MIA not only induced post-acute effects on ERV expression in the placenta and fetal brain, but it also led to lasting but variable effects on these endogenous retroviral elements in the brains of adult offspring. The latter corroborate the findings of Page et al. (2021), demonstrating increased expression of several retrotransposable elements, including elements of the human ERVs and long terminal repeat families in a non-human primate model of MIA. We also found that at least part of the MIA-induced changes in placental and fetal ERV expression correlate with maternal plasma levels of IL-6, a key cytokine implicated in MIA-induced neurodevelopmental disorders (Smith et al., 2007; Hsiao and Patterson, 2011; Aguilar-Valles et al., 2012). The inclusion of maternal IL-6 and its correlation with placental/fetal ERV transcripts have clear translational value, as maternal plasma samples are more easily accessible than placental or fetal samples. Hence, the identified correlations between maternal IL-6 levels and placental and fetal mRNA levels may be used as a proxy to estimate possible changes in placental and fetal ERV transcription whenever maternal IL-6 is analyzed in studies of MIA or other immune-modulating pathologies during pregnancy. Taken together, our data support a role of abnormal expression of endogenous retroviral elements in disease susceptibility in association with MIA. In a broader context, our findings support the hypothesis that ERVs may play a critical role in mediating adaptive phenotypic responses upon environmental inputs (Sharif et al., 2013), including environmental factors affecting prenatal development (Cipriani et al., 2018b; Tartaglione et al., 2019).

There seems to be a bidirectional relationship between ERV expression and inflammation. On the one hand, it has long been recognized that inflammatory stimuli have the potential to trigger ERV expression. In support for this hypothesis, exposure to bacterial endotoxin or specific pro-inflammatory cytokines was found to increase the expression of ERVs in both murine (Kwon et al., 2011) and human (Manghera et al., 2015; 2016) tissues or cells. Our findings are consistent with these findings and show that maternal exposure to a viral-like acute phase response increases mRNA levels of IL-6 and several ERVs in the placenta and, to a somewhat lesser extent, fetal brain. On the other hand, ERVs themselves appear to have pro-inflammatory effects. One of the first studies supporting this hypothesis demonstrated that the human ERV-W envelope (Env) protein is capable of activating the toll-like receptor 4 pathway in human monocytes (Rolland et al., 2006). Similarly, human and rat microglia were found to display elevated pro-inflammatory cytokine and chemokine production after exposure to the human ERV-W Env protein (Kremer et al., 2019; Wang et al., 2021). Using CRISPR/Cas9-based gene disruption of Trim28, which is a key epigenetic co-repressor of ERV expression, Jönsson et al. (2021) recently demonstrated that elevating ERVs causes lasting inflammatory response in mice. Taken together, the current consensus is that while ERVs can trigger inflammatory processes through multiple pathways of the innate and adaptive arms of the immune system, inflammatory signals may drive the (re-)activation and/or maintain the expression of ERVs, leading to a sequence of reciprocal cause and effect (Küry et al., 2018). In line with these relationships, we found positive correlations between IL-6 and several ERV transcripts, both post-acutely after maternal poly(I:C) treatment and in the brains of the adult offspring. Since these findings were correlative in nature, however, future studies will be needed to further dissociate primary versus secondary effects in these associations. It should also be noted that the mean IL-6 expression differences were markedly greater between male CON and MIA offspring as compared to female CON and MIA offspring, both in the fetal brain as well as in the adult mPFC. This relative difference may partly stem from the fact that

the basal gene expression levels of IL-6 were found to be higher in females as compared to males (Suppl. Fig. S4, Suppl. Fig. S5), so that there were comparably weaker MIA-induced increases in IL-6 expression due to ceiling effects in females as compared to males.

An important finding of our study was the identification of subgroup-specific effects of MIA on long-term ERV expression. Consistent with our previous large-scale study (Mueller et al., 2021), we found that offspring of MIA-exposed mothers can be stratified into subgroups that are characterized by the presence (Sus-MIA subgroup) or absence (Res-MIA subgroup) of overt behavioral anomalies at adult age. Intriguingly, the present study further suggests that resilience and susceptibility to MIA is associated with differential expression of ERVs. In line with this hypothesis, male Sus-MIA offspring displayed a consistent increase in the expression of ERVs relative to male CON and/or Res-MIA offspring, whereas male CON and Res-MIA did not differ with regards to the levels of ERV transcripts. These findings provide complementary experimental evidence to recent clinical investigations in humans, suggesting that increased expression of human ERV type W envelope (HERV-W ENV) in schizophrenia and bipolar disorder can be used to stratify patients with major mood and psychotic disorders into subgroups with differing inflammatory and clinical profiles (Tamouza et al., 2021).

Contrary to male offspring, however, there was a a strikingly different pattern of ERV expression in subgroups of MIA-exposed female offspring. Indeed, while the majority of ERV transcripts did not differ between female Sus-MIA and CON offspring, female Res-MIA offspring displayed a marked decrease in the levels of ERV transcripts as compared to female CON and Sus-MIA offspring. Given that IL-6 mRNA levels were increased in male and female Sus-MIA offspring alike, the sex-dependent effects of MIA on subgroup-specific ERV expression seem unrelated to alterations in IL-6 transcription. Hence, molecular mechanisms beyond IL-6 expression are likely to be involved in mediating the differential subgroup-specific expression of ERV in male and female MIA offspring.

On speculative grounds, the sexually dimorphic association with susceptibility and resilience after MIA may be accounted for, at least in part, by the inherent sex differences in basal expression of ERVs. Compared to adult CON males, female CON animals were found to display consistently higher mRNA levels of various ERVs, including ETnI, ETnIIβ, IAP, MusD and SynB (Suppl. Fig. S5). Interestingly, sex-dependent effects have also been identified in peripheral blood mononuclear cells of male and female subjects with regards to the expression of HERV-K elements (Mueller et al., 2018b), which are phylogenetically related to class II murine ERVs (Stocking and Kozak, 2008). These differences may be largely driven by the sex hormones progesterone and estradiol (Mueller et al., 2018b), which have been shown to modulate HERV-K involving binding of progesterone receptor and the octamer-binding transcription factor 4 to HERV-K long terminal repeats (Nguyen et al., 2019). There is also evidence suggesting that Syn1 expression is upregulated by progesterone (Noorali et al., 2009), which in turn may play a role in placentation and maintenance of human pregnancy (Spencer et al., 2007). Likewise, the association between HERV-W expression and worsening of clinical symptoms in patients with multiple sclerosis appears to be influenced by sex (Garcia-Montojo et al., 2013). While an exploration of the mechanisms mediating the observed sex-dependent effects is warranted in future studies, our findings provide initial evidence for a sexually dimorphic role of ERVs in shaping resilience and susceptibility to MIA. Whereas MIA-induced overexpression of ERVs may confer susceptibility to long-term behavioral effects in males, a potentially compensatory and developmentally regulated downregulation of ERVs may protect female MIA offspring from developing overt behavioral anomalies in adult life. We recognize that this hypothesis is entirely speculative at the present stage of investigation, but at the same time, it offers a theoretical framework for future studies aiming to elucidate the molecular mechanisms underlying the sex-specific effects of MIA on ERV expression in behaviorally stratified offspring.

An alternative (but not mutually exclusive) explanation for the present results is that resilience and susceptibility to MIA primarily involves subgroup-specific expression of SynB. Murine SynB (and the human analog, Syn2) is part of the syncytin family of class I retroviral glycoproteins, which are pivotal for placental development and maintenance of pregnancy in multiple species, including rodents and humans (Mi et al., 2000; Dupressoir et al., 2011). In post-miotic tissue, syncytins can act as immunotoxins with superantigen-like effects, thereby activating the innate immune system and inducing inflammatory responses (Wang et al., 2018a; b). Interestingly, increased peripheral and central expression of syncytin transcripts has been found in psychosis-related disorders, including schizophrenia (Huang et al., 2011; Wang et al., 2018a, Li et al., 2019). Here, we found that SynB mRNA was similarly elevated in both male and female Sus-MIA offspring as compared to CON and Res-MIA offspring of the corresponding sex. Moreover, we found that SynB expression correlated inversely with social behavior in males and with PPI in females. Taken together, the subgroup-specific effects of MIA on long-term SynB expression may play an important role in shaping susceptibility to adult behavioral dysfunctions independently of sex.

Contrary to its consequences in the adult brain, however, MIA markedly decreased the expression of SynA and SynB in the placenta. Again, these effects emerged similarly in placental tissue of male and female offspring and correlated inversely with placental IL-6 transcripts. Previous work in animal models suggested that post-acute pathological consequences of MIA involve abnormal placental development (Hsiao and Patterson, 2011; Fatemi et al., 2012; Wu et al., 2017; Núñez Estevez et al., 2020; Creisher et al., 2022), which in turn may induce placental insufficiency and disrupt normal fetal development. In keeping with the pivotal role of syncytins in placental development (Mi et al., 2000; Dupressoir et al., 2011), the MIA-induced decrease in SynA and SynB expression may highlight a novel pathological mechanism by which this early-life adversity can affect normal placental development and functions. Future studies will be needed, however, to test this hypothesis more directly.

We appreciate that our study has some limitations. First, the identified relationships between IL-6 and ERV expression on the one hand, and between abnormal ERV expression and emergence of behavioral dysfunctions on the other hand, are based on correlative evidence only. Hence, future work will be necessary to support causality for these associations. Second, the precise pathophysiological relevance of altered ERV expression in the MIA model remains unknown. The primary reason for this interpretative limitation is that the physiological functions of most murine ERVs are still unknown. With the notable exceptions of SynA and SynB, which are relatively well known for their roles in placental development (Mi et al., 2000; Dupressoir et al., 2011), it would appear challenging to link abnormal expression of specific ERVs to discrete changes in brain and behavior. Third, only two offspring per sex were randomly selected from each MIA litter for the subsequent behavioral and molecular analyses in adulthood, whereas one offspring per sex was randomly selected from each control litter. Hence, unlike before (Mueller et al., 2021), the present study was not based on a whole-litter testing approach, making contrasts between within- and between-litter effects on the stratification of mice into susceptible and resilient subgroups less powerful. Despite the lack of a whole-litter testing approach, however, we found a relatively even distribution of Sus-MIA and Res-MIA offspring across the individual MIA litters, such that each litter contained offspring from both subgroup concomitantly (Suppl. Fig. S3). While this distribution pattern appears to be consistent with our previous findings (Mueller et al., 2021), it should be interpreted with caution, as it is not based on the inclusion of each single offspring from a given litter. Likewise, the molecular investigations of placental and fetal samples were based on a relatively small sample size, whereby only one placental and corresponding fetal sample per sex was randomly selected from each litter. This experimental design prevented us from performing meaningful cluster analyses to explore whether a

proportionality of cluster membership would exist that is comparable to the stratification of adult MIA offspring into susceptible and resilient subgroups. Finally, even though we included both prenatal and adult samples in our study, the developmental trajectories of abnormal ERV expression remains incomplete. Investigating additional timepoints during postnatal brain maturation would be desirable, especially given our findings showing that the directionality of some of the MIA-induced gene expression changes varied between fetal and adult timepoints (Suppl. Fig. S6).

Notwithstanding these limitations, our study identifies post-acute and long-term changes in the expression of endogenous retroviral elements in the poly(I:C)-based MIA model of neurodevelopmental disorders. Our findings thus provide a proof of concept that an inflammatory stimulus, even when initiated in prenatal life, has the potential of altering ERV expression across fetal to adult stages of development. Most importantly, our data further highlight that susceptibility and resilience to MIA, as defined by dissociable behavioral profiles in adulthood, are associated with differential expression of endogenous retroviral elements. Thus, our study provides additional insights into the molecular mechanisms underlying the dissociation of MIA-exposed offspring into susceptible and resilient subgroups. Given that MIA is a noticeable environmental risk factor for psychiatric disorders (Brown and Meyer, 2018), our findings may be taken as experimental evidence suggesting that early-life exposure to inflammatory factors may play a role in determining disease susceptibility by inducing persistent alterations in the expression of endogenous retroviral elements.

Declaration of Competing Interest

The authors declare that they have no known competing financial interests or personal relationships that could have appeared to influence the work reported in this paper.

Data availability

Data will be made available on request.

Acknowledgements

The present study was supported by the Swiss National Science Foundation (grant No. 310030_188524 and 407940_206399 awarded to U.M.; grant No. 310030E_193899, awarded to UWS), the University of Zurich, and the Betty & David Koetser Foundation for Brain Research. PK received grants from Deutsche Forschungsgemeinschaft (DFG; grants KU1934/2-1, KU1934/5-1), Stifterverband/ Novartisstiftung, from the Christiane and Claudia Hempel Foundation for clinical stem cell research and the James and Elisabeth Cloppenburg, Peek and Cloppenburg Düsseldorf Stiftung.

Appendix A. Supplementary data

Supplementary data to this article can be found online at https://doi.org/10.1016/j.bbi.2022.10.006.

References

Aguilar-Valles, A., et al., 2012. Leptin and interleukin-6 alter the function of mesolimbic dopamine neurons in a rodent model of prenatal inflammation. Psychoneuroendocrinology 37, 956–969.
Balestrieri, E., et al., 2012. HERVs expression in autism spectrum disorders. PLoS One 7, e48831.
Balestrieri, E., et al., 2014. Human endogenous retroviruses and ADHD. World J. Biol. Psychiatry 15, 499–504.
Balestrieri, E., et al., 2019a. Children with autism spectrum disorder and their mothers share abnormal expression of selected endogenous retroviruses families and cytokines. Front. Immunol. 10, 2244.
Balestrieri, E., et al., 2019b. Endogenous retroviruses activity as a molecular signature of neurodevelopmental disorders. Int. J. Mol. Sci. 20, 6050.
Baust, C., et al., 2003. Structure and expression of mobile ETnII retroelements and their coding-competent MusD relatives in the mouse. J. Virol. 77, 11448–11458.
Bourque, G., et al., 2018. Ten things you should know about transposable elements. Genome Biol. 19, 199.
Brown, A.S., Meyer, U., 2018. Maternal immune activation and neuropsychiatric illness: a translational research perspective. Am. J. Psychiatry 175, 1073–1083.
Careaga, M., Murai, T., Bauman, M.D., 2017. Maternal immune activation and autism spectrum disorder: from rodents to nonhuman and human primates. Biol. Psychiatry 81, 391–401.
Cipriani, C., et al., 2018a. The decrease in human endogenous retrovirus-H activity runs in parallel with improvement in ADHD symptoms in patients undergoing methylphenidate therapy. Int. J. Mol. Sci. 19, 3286.
Cipriani, C., et al., 2018b. High expression of endogenous retroviruses from intrauterine life to adulthood in two mouse models of autism spectrum disorders. Sci. Rep. 8, 629.
Creisher, P.S., et al., 2022. Downregulation of transcriptional activity, increased inflammation, and damage in the placenta following in utero Zika virus infection is associated with adverse pregnancy outcomes. Front. Virol. 2, 782906.
Dupressoir, A., et al., 2005. Syncytin-A and syncytin-B, two fusogenic placenta-specific murine envelope genes of retroviral origin conserved in Muridae. Proc. Natl. Acad. Sci. USA 102, 725–730.
Dupressoir, A., et al., 2011. A pair of co-opted retroviral envelope syncytin genes is required for formation of the two-layered murine placental syncytiotrophoblast. Proc. Natl. Acad. Sci. USA 108, E1164–E1173.
Fatemi, S.H., et al., 2012. The viral theory of schizophrenia revisited: abnormal placental gene expression and structural changes with lack of evidence for H1N1 viral presence in placentae of infected mice or brains of exposed offspring. Neuropharmacology 62, 1290–1298.
Feschotte, C., Gilbert, C., 2012. Endogenous viruses: insights into viral evolution and impact on host biology. Nat. Rev. Genet. 13, 283–296.
Frank, O., et al., 2005. Human endogenous retrovirus expression profiles in samples from brains of patients with schizophrenia and bipolar disorders. J Virol. 79, 10890–10901.
Garcia-Montojo, M., et al., 2013. The DNA copy number of human endogenous retrovirus-W (MSRV-type) is increased in multiple sclerosis patients and is influenced by gender and disease severity. PLoS One 8, e53623.
Geis, F.K., Goff, S.P., 2020. Silencing and transcriptional regulation of endogenous retroviruses: an overview. Viruses 12, 884.
Hsiao, E.Y., Patterson, P.H., 2011. Activation of the maternal immune system induces endocrine changes in the placenta via IL-6. Brain Behav. Immun. 25, 604–615.
Huang, W., et al., 2011. Implication of the env gene of the human endogenous retrovirus W family in the expression of BDNF and DRD3 and development of recent-onset schizophrenia. Schizophr. Bull. 37, 988–1000.
Jönsson, M.E., et al., 2021. Activation of endogenous retroviruses during brain development causes an inflammatory response. EMBO J. 40, e106423.
Karlsson, H., et al., 2004. HERV-W-related RNA detected in plasma from individuals with recent-onset schizophrenia or schizoaffective disorder. Mol. Psychiatry 9, 12–13.
Kassiotis, G., 2014. Endogenous retroviruses and the development of cancer. J. Immunol. 192, 1343–1349.
Kentner, A.C., et al., 2019. Maternal immune activation: reporting guidelines to improve the rigor, reproducibility, and transparency of the model. Neuropsychopharmacology 44, 245–258.
Kremer, D., et al., 2019. pHERV-W envelope protein fuels microglial cell-dependent damage of myelinated axons in multiple sclerosis. Proc. Natl. Acad. Sci. USA 116, 15216–15225.
Küry, P., et al., 2018. Human endogenous retroviruses in neurological diseases. Trends Mol. Med. 24, 379–394.
Kwon, D.N., et al., 2011. Lipopolysaccharide stress induces cell-type specific production of murine leukemia virus type-endogenous retroviral virions in primary lymphoid cells. J. Gen. Virol. 92, 292–300.
Labouesse, M.A., et al., 2018. Striatal dopamine 2 receptor upregulation during development predisposes to diet-induced obesity by reducing energy output in mice. Proc. Natl. Acad. Sci. USA 115, 10493–10498.
Lambert, J.F., et al., 2000. Quick sex determination of mouse fetuses. J. Neurosci. Methods. 95, 127–132.
Lander, E.S., et al., 2001. Initial sequencing and analysis of the human genome. Nature 409, 860–921.
Li, F., et al., 2019. Transcription of human endogenous retroviruses in human brain by RNA-seq analysis. PLoS One 14, e0207353.
Livak, K.J., Schmittgen, T.D., 2001. Analysis of relative gene expression data using real-time quantitative PCR and the 2−ΔΔ CT method. Methods 25, 402–408.
Lueders, K.K., Kuff, E.L., 1980. Intracisternal A-particle genes: identification in the genome of Mus musculus and comparison of multiple isolates from a mouse gene library. Proc. Natl. Acad. Sci. USA 77, 3571–3575.
Mager, D.L., Freeman, J.D., 2000. Novel mouse type D endogenous proviruses and ETn elements share long terminal repeat and internal sequences. J. Virol. 74, 7221–7229.
Maksakova, I.A., et al., 2006. Retroviral elements and their hosts: insertional mutagenesis in the mouse germ line. PLoS Genet. 2, e2.
Manghera, M., et al., 2016. NF-kappaB and IRF1 induce endogenous retrovirus K expression via interferon-stimulated response elements in its 5' long terminal repeat. J. Virol. 90, 9338–9349.
Manghera, M., Ferguson, J., Douville, R., 2015. ERVK polyprotein processing and reverse transcriptase expression in human cell line models of neurological disease. Viruses 7, 320–332.
Meyer, U., 2014. Prenatal poly(I:C) exposure and other developmental immune activation models in rodent systems. Biol. Psychiatry 75, 307–315.

Meyer, U., 2019. Neurodevelopmental resilience and susceptibility to maternal immune activation. Trends Neurosci. 42, 793–806.
Meyer, U., Feldon, J., Fatemi, S.H., 2009. In-vivo rodent models for the experimental investigation of prenatal immune activation effects in neurodevelopmental brain disorders. Neurosci. Biobehav. Rev. 33, 1061–1079.
Mi, S., et al., 2000. Syncytin is a captive retroviral envelope protein involved in human placental morphogenesis. Nature 403, 785–789.
Misiak, B., Ricceri, L., Sąsiadek, M.M., 2019. Transposable elements and their epigenetic regulation in mental disorders: Current evidence in the field. Front. Genet. 10, 580.
Mueller, F.S., et al., 2018a. Mouse models of maternal immune activation: Mind your caging system! Brain Behav. Immun. 73, 643–660.
Mueller, O., et al., 2018b. Expression of human endogenous retroviruses in peripheral leukocytes during the menstrual cycle suggests coordinated hormonal regulation. AIDS Res. Hum. Retroviruses 34, 909–911.
Mueller, F.S., et al., 2019. Influence of poly(I:C) variability on thermoregulation, immune responses and pregnancy outcomes in mouse models of maternal immune activation. Brain Behav. Immun. 80, 406–418.
Mueller, F.S., et al., 2021. Behavioral, neuroanatomical, and molecular correlates of resilience and susceptibility to maternal immune activation. Mol. Psychiatry 26, 396–410.
Nguyen, T.D., et al., 2019. Female sex hormones activate human endogenous retrovirus type K through the OCT4 transcription factor in T47D breast cancer cells. AIDS Res. Hum. Retroviruses 35, 348–356.
Noorali, S., et al., 2009. Role of HERV-W syncytin-1 in placentation and maintenance of human pregnancy. Appl. Immunohistochem. Mol. Morphol. 17, 319–328.
Notter, T., et al., 2021. Neuronal activity increases translocator protein (TSPO) levels. Mol. Psychiatry 26, 2025–2037.
Núñez Estevez, K.J., et al., 2020. Environmental influences on placental programming and offspring outcomes following maternal immune activation. Brain Behav. Immun. 83, 44–55.
Page, N.F., et al., 2021. Alterations in retrotransposition, synaptic connectivity, and myelination implicated by transcriptomic changes following maternal immune activation in nonhuman primates. Biol. Psychiatry 89, 896–910.
Perron, H., et al., 2008. Endogenous retrovirus type W GAG and envelope protein antigenemia in serum of schizophrenic patients. Biol. Psychiatry 64, 1019–1023.
Perron, H., et al., 2012. Molecular characteristics of Human Endogenous Retrovirus type-W in schizophrenia and bipolar disorder. Transl. Psychiatry 2, e201.
Pollak, D.D., Weber-Stadlbauer, U., 2020. Transgenerational consequences of maternal immune activation. Semin. Cell. Dev. Biol. 97, 181–188.
Rolland, A., et al., 2006. The envelope protein of a human endogenous retrovirus-W family activates innate immunity through CD14/TLR4 and promotes Th1-like responses. J. Immunol. 176, 7636–7644.
Schubert, D., Martens, G.J., Kolk, S.M., 2015. Molecular underpinnings of prefrontal cortex development in rodents provide insights into the etiology of neurodevelopmental disorders. Mol. Psychiatry 20, 795–809.
Sharif, J., Shinkai, Y., Koseki, H., 2013. Is there a role for endogenous retroviruses to mediate long-term adaptive phenotypic response upon environmental inputs? Philos. Trans. R. Soc. Lond. B Biol. Sci. 368, 20110340.
Silverman, J.L., et al., 2010. Behavioural phenotyping assays for mouse models of autism. Nat. Rev. Neurosci. 11, 490–502.
Slokar, G., Hasler, G., 2016. Human endogenous retroviruses as pathogenic factors in the development of schizophrenia. Front. Psychiatry 6, 183.
Smith, S.E., et al., 2007. Maternal immune activation alters fetal brain development through interleukin-6. J. Neurosci. 27, 10695–10702.
Spencer, T.E., et al., 2007. Pregnancy recognition and conceptus implantation in domestic ruminants: roles of progesterone, interferons and endogenous retroviruses. Reprod. Fertil. Dev. 19, 65–78.
Stocking, C., Kozak, C.A., 2008. Murine endogenous retroviruses. Cell. Mol. Life Sci. 65, 3383–3398.
Tamouza, R., et al., 2021. Identification of inflammatory subgroups of schizophrenia and bipolar disorder patients with HERV-W ENV antigenemia by unsupervised cluster analysis. Transl. Psychiatry 11, 377.
Tartaglione, A.M., et al., 2019. Early behavioral alterations and increased expression of endogenous retroviruses are inherited across generations in mice prenatally exposed to valproic acid. Mol. Neurobiol. 56, 3736–3750.
Tovo, P.A., et al., 2022. Enhanced expression of human endogenous retroviruses, TRIM28 and SETDB1 in autism spectrum disorder. Int. J. Mol. Sci. 23, 5964.
Volkman, H.E., Stetson, D.B., 2014. The enemy within: endogenous retroelements and autoimmune disease. Nat. Immunol. 15, 415–422.
Wang, X., et al., 2018a. Syncytin-1, an endogenous retroviral protein, triggers the activation of CRP via TLR3 signal cascade in glial cells. Brain Behav. Immun. 67, 324–334.
Wang, X., et al., 2021. Human endogenous retrovirus W family envelope protein (HERV-W env) facilitates the production of TNF-α and IL-10 by inhibiting MyD88s in glial cells. Arch. Virol. 166, 1035–1045.
Wang, X., Huang, J., Zhu, F., 2018b. Human endogenous retroviral envelope protein syncytin-1 and inflammatory abnormalities in neuropsychological diseases. Front. Psychiatry. 9, 422.
Waterston, R.H., et al., 2002. Initial sequencing and comparative analysis of the mouse genome. Nature 420, 520–562.
Weber-Stadlbauer, U., et al., 2017. Transgenerational transmission and modification of pathological traits induced by prenatal immune activation. Mol. Psychiatry. 22, 102–112.
Weber-Stadlbauer, U., Meyer, U., 2019. Challenges and opportunities of a-priori and a-posteriori variability in maternal immune activation models. Curr. Opin. Behav. Sci. 28, 119–128.
Wicker, T., et al., 2007. A unified classification system for eukaryotic transposable elements. Nat. Rev. Genet. 8, 973–982.
Wu, W.L., et al., 2017. The placental interleukin-6 signaling controls fetal brain development and behavior. Brain Behav Immun. 2017 May;62:11–23.
Yao, Y., et al., 2008. Elevated levels of human endogenous retrovirus-W transcripts in blood cells from patients with first episode schizophrenia. Genes Brain Behav. 7, 103–112.